

Transitions between polarization and radicalization in a temporal bilayer echo-chamber modelŁukasz G. Gajewski * and Julian Sienkiewicz *Faculty of Physics, Warsaw University of Technology, Koszykowa 75, 00-662 Warszawa, Poland*Janusz A. Hołyst *Faculty of Physics, Warsaw University of Technology, Koszykowa 75, 00-662 Warszawa, Poland
and ITMO University, Kronverkskiy Prospekt 49, St. Petersburg, 197101 Russia*

(Received 11 November 2021; accepted 3 February 2022; published 18 February 2022)

Echo chambers and polarization dynamics are, as of late, a very prominent topic in scientific communities around the world. As these phenomena directly affect our lives, seemingly more and more as our societies and communication channels evolve, it becomes ever so important for us to understand the intricacies of opinion dynamics in the modern era. Here we extend an existing echo-chamber model with activity-driven agents to a bilayer topology and study the dynamics of the polarized state as a function of interlayer couplings. Different cases of such couplings are presented: unidirectional coupling that can be reduced to a monolayer facing an external bias and symmetric and nonsymmetric couplings. We have assumed that initial conditions impose system polarization and agent opinions are different for both layers. Such a preconditioned polarized state can persist without explicit homophilic interactions provided the coupling strength between agents belonging to different layers is weak enough. For a strong unidirectional or attractive coupling between two layers a discontinuous transition to a radicalized state takes place when mean opinions in both layers are the same. When coupling constants between the layers are of different signs, the system exhibits sustained or decaying oscillations. Transitions between these states are analyzed using a mean field approximation and classified in the framework of bifurcation theory.

DOI: [10.1103/PhysRevE.105.024125](https://doi.org/10.1103/PhysRevE.105.024125)**I. INTRODUCTION**

It is not unheard of in the scientific community to attempt to model how our societies form and function using techniques and approaches familiar to physicists [1–5]. Of particular interest lately has been the dynamics of opinion formation, especially in light of recently better studied phenomena such as echo chambers [6–9] and misinformation [10–15]. One of the major effects that seems to be strongly connected with echo chambers and misinformation is that of polarization. While not every topic is polarizing [16,17], many certainly can be [7,18–25]. It seems to have been recognized by some that polarization is dangerous to the state of democracy around the world and that there is a need for research on this topic [26–32], especially in light of the possible event of democracy backsliding [33,34].

We find that it is also of interest to study the possible dynamics between two clearly defined groups, which often can be found in politics (e.g., Democrats vs Republicans in the United States) and particular topics (pro vs anti) and has precedence in sociophysics [35–41]. In particular we felt inspired by the work of Baumann *et al.* [6] in which the authors introduced an echo-chamber and polarization model on complex networks. In this paper we modify said model so that it operates on a bilayer temporal network, as opposed to

a monolayer, where each layer can represent a clearly defined group of individuals (agents). This transformation is directly driven by the fact that the physical properties of many systems drastically change (e.g., phase transition type change) when considered on a duplex (bilayer) topology [42,43]. We show that several complex behaviors can be acquired by simply changing the nature of the coupling between those layers. Let us underline that the question of interacting layers is an extremely vivid topic in the view of the COVID-19 epidemic (or infodemic [44]). Recent studies point to a pivotal role played by the risk perception layer in the spreading of a disease [45] or, explicitly, the attitude toward vaccination [46]. In this scope examining the dynamics of two *coupled* opposite groups (e.g., pro- and anti-vaccination [47]) seems to be highly relevant.

Originally, in the work of Baumann *et al.*, the system consisted of N agents, each with a real, continuous opinion variable $x_i(t) \in \mathbb{R}$. The sign determines the nature of opinion (for or against), while the value determines the conviction to it. The opinion dynamics is driven exclusively by the interactions between agents and is described by the system of coupled ordinary differential equations presented in [6]:

$$\dot{x}_i = -x_i + K \sum_{j=1}^N A_{ij}(t) \tanh(\alpha x_j), \quad (1)$$

where $K > 0$ is the *social interaction strength* and $\alpha > 0$ determines the degree of nonlinearity. The rationale behind

*lukaszgajewski@tuta.io

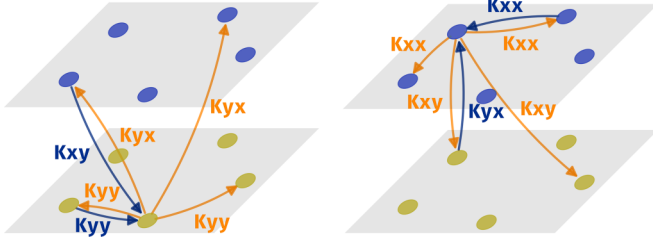


FIG. 1. Illustration of the temporal bi-layer network model. At any given moment an agent from either group can get activated and impose its influence upon other (orange/light arrows) while in some cases this influence can be reciprocated (blue/dark arrows). Each arrow is labelled with an appropriate social influence coefficient later on used in system of equations (3).

this very equation is built on the mechanism of informational influence theory with guarantees of monotonic influence and a cap on extreme opinions and is also not dissimilar to previously used nonlinear functions in chaotic systems [48–51]. The matrix A is an $N \times N$ adjacency matrix in an activity-driven (AD) temporal network model [52–55] (see Fig. 1 for our bilayer interpretation). This is a model without a statically set social network, but in each time step an agent can become active with *propensity* $a_i \in [\epsilon, 1]$. The propensities are drawn from a power law distribution [52,54] defined as follows:

$$F(a) = \frac{1 - \gamma}{1 - \epsilon^{1-\gamma}} a^{-\gamma}. \quad (2)$$

Once the agent is activated, it makes m random connections with other agents, and as is standard in AD models, the connections are uniformly random. In [6] there is additionally an element of homophily because it is expected to be necessary

$$\begin{aligned} \dot{x}_i &= -x_i + K_{xx} \sum_j^{N_x} A_{ij}^{xx}(t) \tanh(\alpha_{xx} x_j) + K_{xy} \sum_j^{N_y} A_{ij}^{xy}(t) \tanh(\alpha_{xy} y_j), \\ \dot{y}_i &= -y_i + K_{yy} \sum_j^{N_y} A_{ij}^{yy}(t) \tanh(\alpha_{yy} y_j) + K_{yx} \sum_j^{N_x} A_{ij}^{yx}(t) \tanh(\alpha_{yx} x_j). \end{aligned} \quad (3)$$

This is the most general formulation of the model we propose, and we will now appropriately simplify it and later on discuss its various regimes and the scenarios that emerge from it.

Let us further assume that $K_{xx} = K_{yy} = K$, $\alpha_{xx} = \alpha_{yy} = \alpha_{xy} = \alpha_{yx} = \alpha$, $N_x = N_y = \frac{1}{2}N$, and both r and a are the same for both groups, within as well as without. Average activity is given by

$$\langle a \rangle = \frac{1 - \gamma}{2 - \gamma} \frac{1 - \epsilon^{2-\gamma}}{1 - \epsilon^{1-\gamma}}. \quad (4)$$

Like in [6], we assume that processes related to topology changes as described by matrices $A_{ij}(t)$ are much faster than changes of opinions $x_i(t)$ and $y_i(t)$, and we shall insert into (3) mean values of these matrices $\langle A_{ij}(t) \rangle_{t,a} = \frac{1}{2}m(1+r)\langle a \rangle$ (see the section ‘‘Approximation of the Critical Controversialness’’ in the Supplemental Material of [6] for a detailed derivation). When $K_{xy} = K_{yx}$, then the Jacobian of (3) calculated at the

to create polarization effects [56,57]; however, since we will be considering a bilayer model later on, that is not the case for us. A proper study of the effects of the homophily in the from presented by Baumann *et al.* could turn out to be of interest, yet we find it goes beyond the scope of this paper.

Interactions on social media can often be asymmetric, so it is not always true that $A_{ij} = A_{ji}$. However, in this model there is a mechanism of *reciprocity* in which each agent j that has received a connection from an active agent i can reciprocate the connection with probability r .

Following the terminology from the paper [6], we will name three specific opinion distributions as follows: (i) a *neutral consensus* (or, simply, consensus) will correspond to a phase when agents’ opinions in both layers are similar and, on average, are close to zero; (ii) a *one-side radicalization* (OSR; or, simply, radicalization) will be the opinion distribution when in both layers either a positive or a negative opinion is overwhelming and is the same in both layers; and (iii) a *polarization* will be the opinion distribution when in one layer a positive opinion is overwhelming but in the other layer the negative opinion is overwhelming. Using the language of magnetic systems the neutral consensus corresponds to the paramagnetic phase, the radicalization is the ferromagnetic phase, and the polarization is the antiferromagnetic phase [58].

II. MODEL DESCRIPTION

We modify the scenario described by Baumann *et al.* by considering a system of two (potentially) opposing groups represented by layers X and Y such that N_x agents belong to group X and N_y belong to Y . With this (1) becomes

point $x_i = y_i = 0$ possesses two special eigenvectors, $e_+ = [1, 1, 1, \dots, 1, 1, 1]^T$ and $e_- = [1, 1, 1, \dots, -1, -1, -1]^T$, and the corresponding eigenvalues $\lambda_+ = c\alpha[K(N_x - 1)/N_x + K_{xy}]$ and $\lambda_- = c\alpha[K(N_x - 1)/N_x - K_{xy}]$.

Then we can write the mean field equations for the expected values of opinions in X and Y . For simplicity let us set $c = \frac{m}{2}(1+r)\langle a \rangle$, and then

$$\begin{aligned} \langle \dot{x} \rangle &= -\langle x \rangle + Kc \tanh(\alpha \langle x \rangle) + K_{xy}c \tanh(\alpha \langle y \rangle), \\ \langle \dot{y} \rangle &= -\langle y \rangle + Kc \tanh(\alpha \langle y \rangle) + K_{yx}c \tanh(\alpha \langle x \rangle). \end{aligned} \quad (5)$$

We show that in our bilayer variant of the echo-chamber and polarization model [6], when initial conditions impose a polarized state and there are opposite agents’ opinions in different layers, depending on the type of interlayer coupling, various patterns are observed. For a weak attractive coupling the polarized state is preserved, but when the coupling reaches

a critical value a discontinuous transition to a radicalization phase [6,59,60] takes place, and opinions in both layers are similar and biased towards a positive or negative value. An asymmetric (attractive or repulsive) coupling between agents in both layers induces oscillations of opinions.

Let us stress that when the coupling between layers is weak, the layers operate independently, and each of them becomes an analog to the system studied in [6] when the homophily is neglected. Thus, each given layer can be radicalized, but the composite bilayer system can also be *polarized* when each layer has its own radicalized state *opposite* to the other layer's (this opposition state depends on the initial conditions, however).

Later on, we provide agent-based simulations and detailed mathematical analysis that makes use of the mean field approximation and catastrophe theory and fits well to results of agent-based numerical simulations.

Our work is also distinctly different from the recent publication of Baumann *et al.* [26], in which the authors considered a multidimensional version of the echo-chamber model. In their work the coupling occurs via a correlated *topic* space, whereas we establish a variant with *interacting groups*, quite naturally leading to very different phenomena being observed.

III. METHODOLOGY

All simulations were conducted, unless stated otherwise, with parameter values: network size $N = 1000$, $\gamma = 2.1$, $\epsilon = 0.01$, $m = 10$, $r = 0.5$, $K = 1$, $\alpha = 1$, $K_{xy} = K_{yx} = -1$ (or 1, -1 accordingly in the asymmetric, oscillating case and 1,1 in the positive symmetric, weak coupling case). Note that as a consequence of these values, the parameter $c \approx 0.306$. The systems of equations in the agent-based simulations were integrated using an explicit fourth order Runge-Kutta method with a time step $dt = 0.05$. The temporal adjacency matrix A_{ij} is computed at each integration step. Mean field equations for which no analytical solution was possible were integrated using an embedded Runge-Kutta 5(4) [61,62]. Following the rationale in [6,63], the AD network is updated in each integration step to separate the timescales of connections and opinion dynamics.

IV. RESULTS

In this section we present the results of agent-based simulations and the mean field approximation for the three scenarios described before. The scenarios are (i) unidirectional coupling (this case will be equivalent to an external bias), (ii) symmetric coupling, (iii) nonsymmetric coupling.

A. Unidirectional coupling

We can study the cumulative effect of a bilayer environment via the addition of external bias to a monolayer system. This bias can represent the cumulative effect of another group (Y) or just the medium in which the system operates.

In essence, stemming from Eq. (3), we set $K_{yx} = 0$, $K_{xx} = K \neq K_{yy}$, $\alpha_{xx} = \alpha \neq \alpha_{yy} \neq \alpha_{yx} \neq \alpha_{xy}$. If $K_{yy}\alpha_{yy}c > 1$, then layer Y is radicalized, and agents' opinions y_i in this layer are centered around a certain nonzero value $\langle y \rangle$ that is constant in time. In such a case the whole term

$K_{xy} \sum_j^{N_y} A_{ij}^{xy}(t) \tanh(\alpha_{xy}y_j) = B_i$ can be "hidden" behind a cumulative effect: an external bias B_i that can be, in general, dependent on the site i and can either support a local opinion x_i in layer X or work in opposition to x_i .

Therefore, we can write

$$\dot{x}_i = -x_i + K \sum_j^N A_{ij}(t) \tanh(\alpha x_j) + B_i, \quad (6)$$

and by averaging x_i we get

$$\langle \dot{x} \rangle = -\langle x \rangle + Kc \tanh(\alpha \langle x \rangle) + B, \quad (7)$$

where $B = \langle B_i \rangle$. The dynamical system described by (7) exhibits a cusp catastrophe [64,65]. If $Kc\alpha < 1$, then there is only one steady state solution of (7). However, if $Kc\alpha > 1$, then two scenarios are possible. When the modulus of the external bias B is smaller than some critical value B_c , Eq. (7) possesses two stable and one unstable fixed points. This means the mean opinion in layer X is in agreement or in disagreement with the external bias B . When B is larger than some critical B_c , Eq. (7) possesses only one solution, and the mean opinion in group X directed against the external bias B is not possible. This means that at some critical B_c a discontinuous transition takes place [see Fig. 2(a)]. Values of B_c can be found from the stability analysis of (6) or (7).

In the case of (7) we get the Lyapunov exponent [66] at point x_c , which corresponds to a steady state solution whose stability is examined,

$$\lambda = -1 + Kc\alpha \operatorname{sech}^2(\alpha x_c). \quad (8)$$

In the case of (6) the Jacobian becomes

$$J|_{x_i=x_c} = \begin{bmatrix} -1 & Kc\alpha \operatorname{sech}^2(\alpha x_c) & \dots \\ Kc\alpha \operatorname{sech}^2(\alpha x_c) & -1 & \dots \\ \vdots & \vdots & \ddots \end{bmatrix}, \quad (9)$$

with the largest eigenvalue being

$$\lambda_{\max} = -1 + \frac{N-1}{N} Kc\alpha \operatorname{sech}^2(\alpha x_c). \quad (10)$$

When $N \rightarrow \infty$, solutions (8) and (10) coincide. Combining the condition for the steady state of (7) and the condition for changing the sign of the eigenvalue λ_{\max} (10), we get a solution for the critical value of the external bias B_c :

$$x_c = \frac{1}{\alpha} \cosh^{-1} \left(\sqrt{\frac{N-1}{N} Kc\alpha} \right) \stackrel{N \rightarrow \infty}{\sim} \frac{1}{\alpha} \cosh^{-1}(\sqrt{Kc\alpha}),$$

$$B_c = x_c - Kc \tanh(\alpha x_c). \quad (11)$$

In order to explore the behavior of Eq. (6) we can examine the effective potential

$$V(x) = - \int_{-\infty}^x F(u) du, \quad (12)$$

where $F(x)$ is the so-called effective force, which is the right-hand side of Eq. (6). Thus, in our case

$$V(x) = \frac{x^2}{2} - \frac{Kc}{\alpha} \ln \cosh(\alpha x) - Bx. \quad (13)$$

If $B = 0$ [Fig. 2(b)], then the potential $V(x)$ is a symmetric function possessing two minimum values and one maximum,

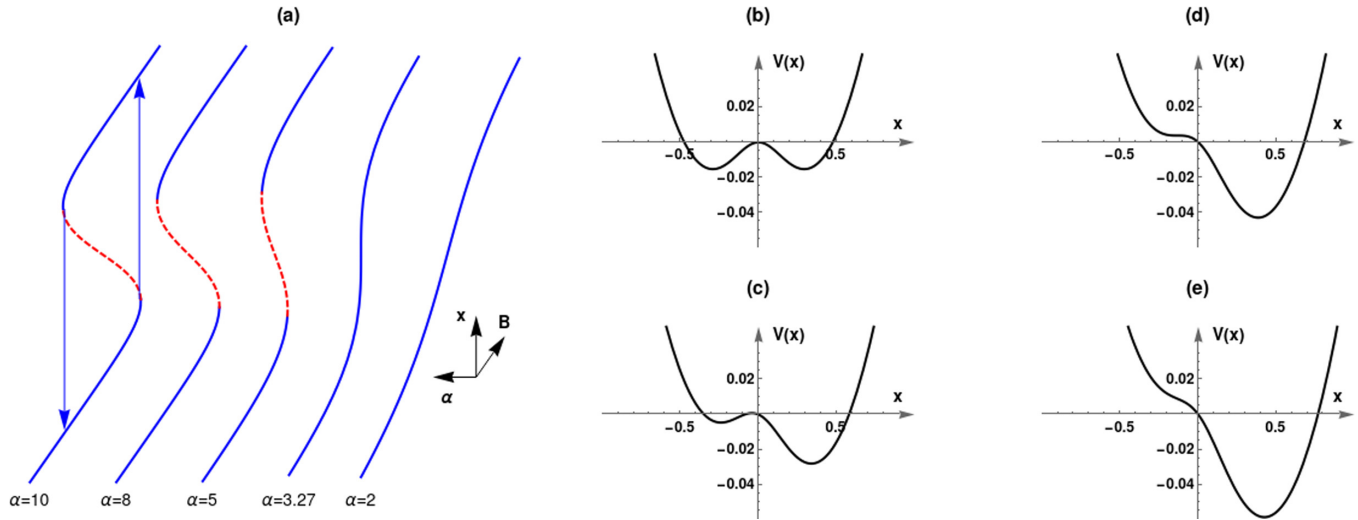


FIG. 2. (a) Bifurcation and hysteresis loop in the system of external bias: for $\alpha > 1/(Kc) \approx 3.27$ the system can be bistable, and once a critical value of B_c is reached, there is a switch of opinion majority from a state against the field to a state towards it (and vice versa for $-B_c$). Also in such a case, we cannot reach a neutral solution ($x = 0$) for any $B > 0$. For $\alpha < 1/(Kc)$ we have only one stable solution, and such effects do not take place. (b)–(e) Shape of the potential $V(x)$ given by Eq. (13) for $Kc\alpha = 2$ and (b) $B = 0$, (c) $B = 0.04$, (d) $B = 0.0815$, and (e) $B = 0.12$.

corresponding to, respectively, stable and unstable solutions, as long as $\alpha > 1/(Kc)$ or one minimum at $x = 0$ if this condition is not fulfilled. However, if $B \neq 0$, the potential becomes asymmetric [Fig. 2(c)], and for $B \geq B_c$ the second minimum is no longer observed [see Figs. 2(d) and 2(e)]. Let us note that if $Kc\alpha \gg 1$ in Eq. (11), then $B_c \rightarrow -Kc$.

The above results mean that a discontinuous phase transition in the temporary network (6) should occur from a system’s steady state to another one that is directed towards the external bias. For example, if the system converges on a negative (average) opinion and we set the bias to a positive and sufficiently large value, the system will suddenly jump to the opposite side. In Fig. 3(a) we present an example of that. We wait until the system reaches its steady state and then activate the bias with an opposite sign. If the value is

below the critical one, the system merely shifts slightly towards zero; however, if $|B| > B_c$, a sudden jump occurs. In Fig. 3(b) we show this in the $B - \alpha$ phase space: yet again, the mean field approach [Eq. (11)] allows us to predict this behavior.

We consider this case study to be illustrative of how, for example, propaganda may or may not be successful. We use “propaganda” here as a neutral term, without concerning ourselves with whether it is good or bad. One can easily imagine situations that are either. Such a scenario boils down to the strength of the campaign in question since the dynamic of change is nonlinear and the transition can be very sudden. One of the significant implications of this is that it may be rather difficult to react to the propaganda machine in time to stop society from drastically shifting its stance.

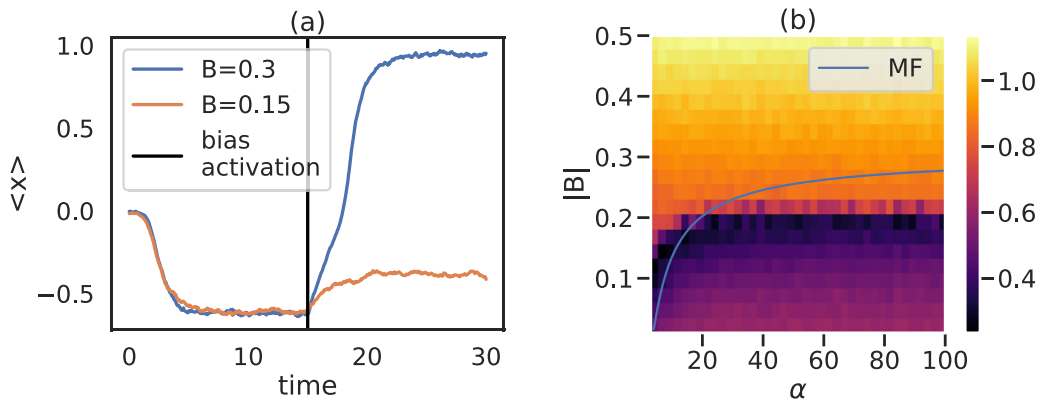


FIG. 3. Phase transition for the temporary network described by (6) under the influence of an external bias. (a) Two examples of an average opinion of the system as a function of time. One trajectory is for a value of external bias above the critical threshold, and the other is for external bias below it. The solid vertical line signifies the moment we enable the external bias. (b) The $B - \alpha$ phase space, where color is $\langle |opinion| \rangle$, with a visible phase transition to an opposite opinion and the mean field approximation for the critical line [Eq. (11)].

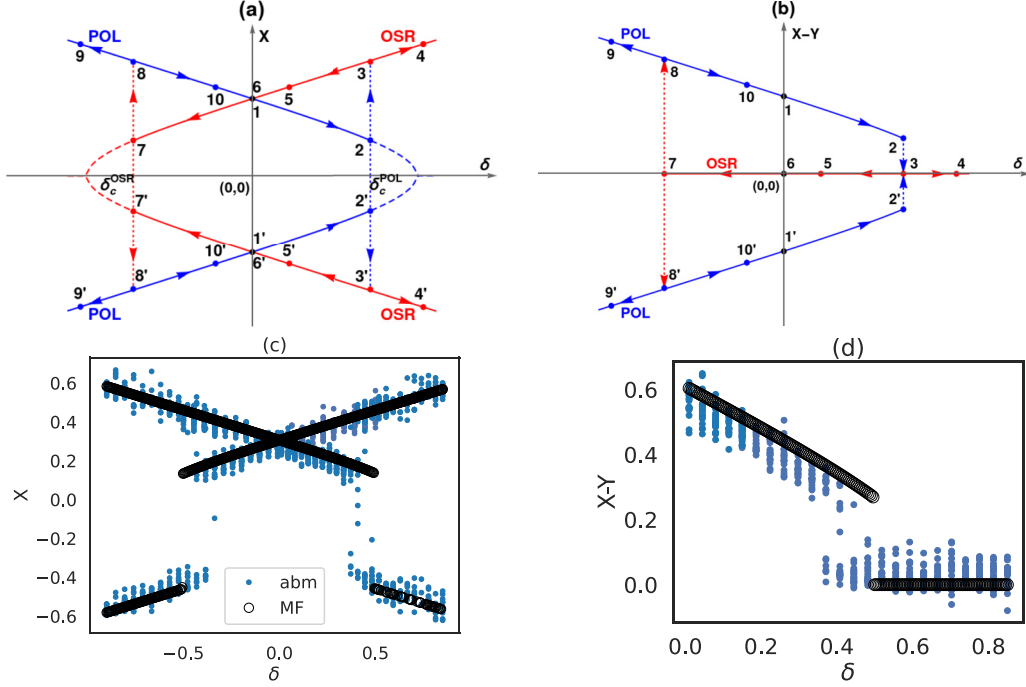


FIG. 4. Illustrations of the phase transition in a weakly coupled scenario for different values of δ in the (a) X, δ and (b) $X - Y, \delta$ planes; see the text for detailed description of points 1–10 and 1' – 10'. (c) and (d) Comparison of analytical predictions with ABM simulations. Dots show 20 independent realizations of an agent-based simulation, while the mean field solution is shown by open circles (with $\alpha = 10$). In (c) only the average opinion of layer X is shown (Y is omitted for clarity as it would simply be symmetrically opposite).

B. Symmetric coupling

Here we consider a variant of the model in which the two layers are positively but weakly coupled via the coupling parameter δ . We introduce this weak coupling parameter $0 < \delta < 1$ to the variant where both K_{xy} and K_{yx} are positive, and for simplicity let us assume $K_{xy} = K_{yx} = \delta K$. Note that for large positive coupling $\delta > 1$ the system functionally reduces to the scenario already described by Baumann *et al.* and therefore will not be discussed by us. The mean field equations for

the expected values can be written as

$$\begin{aligned} \dot{\langle x \rangle} &= -\langle x \rangle + Kc \tanh(\alpha \langle x \rangle) + \delta Kc \tanh(\alpha \langle y \rangle), \\ \dot{\langle y \rangle} &= -\langle y \rangle + Kc \tanh(\alpha \langle y \rangle) + \delta Kc \tanh(\alpha \langle x \rangle). \end{aligned} \quad (14)$$

With positive coupling the two groups ought to merge for some critical value δ_c . However, before that happens the coexistence of two groups with opposite opinions is possible. In such a case $x_c = -y_c$ in the steady state, and by writing out the Jacobian of the system (14)

$$J|_{\langle x \rangle = -\langle y \rangle = x_c} = \begin{bmatrix} -1 + Kc \alpha \operatorname{sech}^2(\alpha x_c) & \delta Kc \alpha \operatorname{sech}^2(\alpha x_c) \\ \delta Kc \alpha \operatorname{sech}^2(\alpha x_c) & -1 + Kc \alpha \operatorname{sech}^2(\alpha x_c) \end{bmatrix}, \quad (15)$$

from which we get both eigenvalues as

$$\lambda_{1,2} = Kc \alpha \operatorname{sech}^2(\alpha x_c) (1 \pm \delta) - 1, \quad (16)$$

and by looking at the largest eigenvalue and the steady state solution, it is easy to find that

$$\begin{aligned} \delta_c &= \frac{1}{Kc \alpha} \cosh^2(\alpha x_c) - 1, \\ 0 &= -x_c + Kc (1 - \delta_c) \tanh(\alpha x_c), \end{aligned} \quad (17)$$

which must be solved numerically.

We find that there exists a critical value δ_c for which a phase transition occurs from a polarization (denoted POL) state to a non-neutral consensus state (or the so-called one-side radicalization).

Figure 4 illustrates this behavior via plots of the (x, δ) and $(x - y, \delta)$ planes with points 1–10 and, equivalently, 1' – 10' referring to specific states of the system. The two layers start in opposition, i.e., in a polarized state (for $\delta = 0$, either point 1 or 1', depending on the setting); then we enable a positive but weak $0 < \delta < 1$ coupling between them. As δ increases, the groups' final average opinions slowly and smoothly approach each other until the critical value of δ_c^{POL} (2 or 2') corresponds to a bifurcation point, where two groups merge into one with a radicalized opinion (3 or 3'). Further increasing δ results in stronger radicalization (4 or 4'). On the other hand, if we follow the path of decreasing δ , the average opinion value drops (5 or 5'), and we arrive once again at $\delta = 0$ (6 or 6'). Although the value of x at point 6 is the same as at point 1, it is a different state, as confirmed

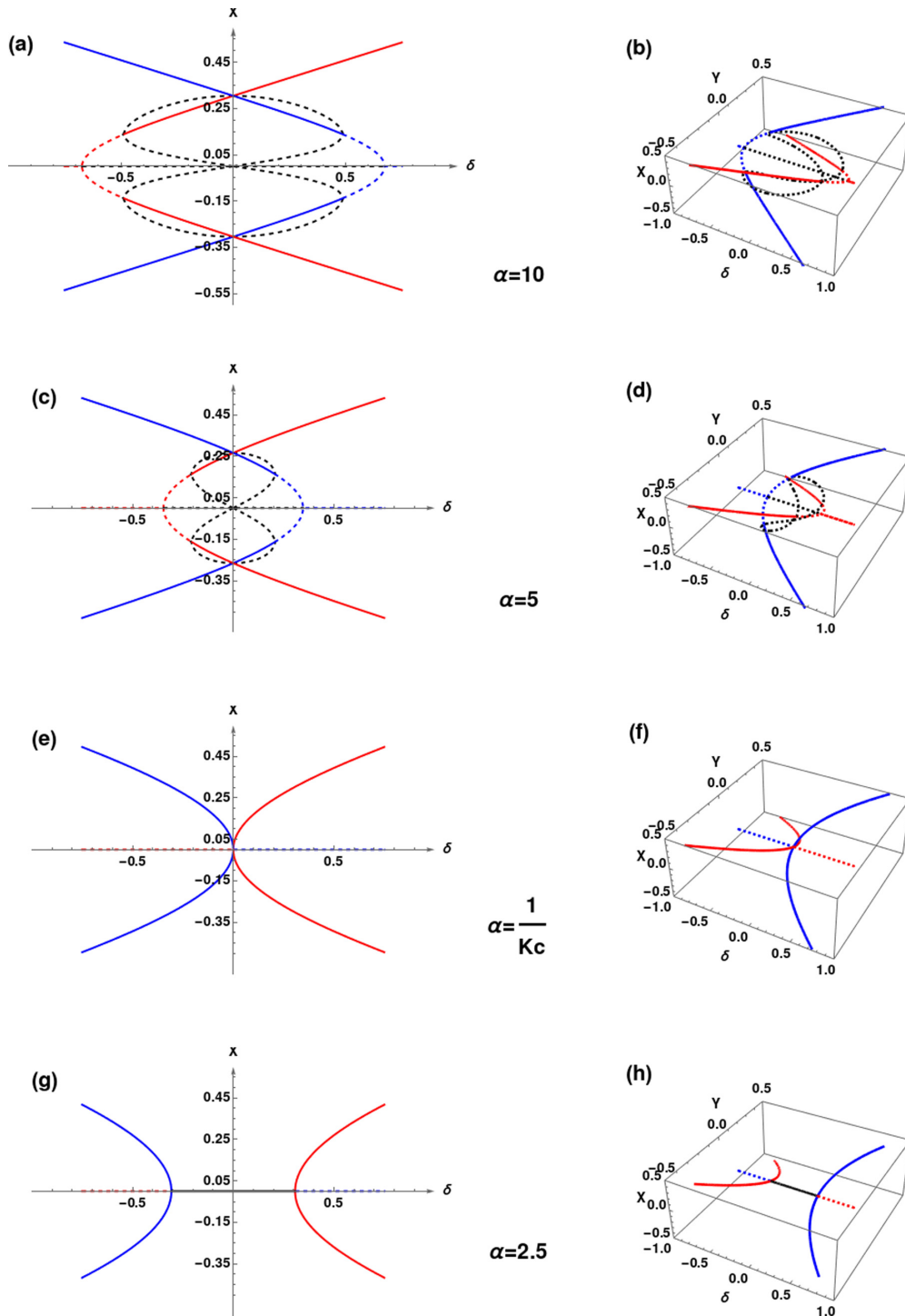


FIG. 5. Solutions of Eq. (3) for different values of α (in each case $K = 1$ and $c = 0.306$); the left column shows x as a function of δ , while the right one shows x, y as a function of δ . Solid lines represent stable solutions, and dotted lines represent unstable solutions. Red and blue curves denote radicalization and polarization (as in Fig. 4); black dashed lines show auxiliary solutions, and black solid lines show neutral consensus.

by Fig. 4(b). We might then keep on decreasing δ , switching to negative values (weak negative coupling) until we reach $\delta_c^{\text{OSR}} = -\delta_c^{\text{POL}}$ at point 7 or 7', which once again corresponds to a bifurcation point, this time leading to a separation of the groups (8 or 8'), i.e., to a POL state. A further decrease of δ strengthens group polarization (9 or 9'), while by increasing it we go through point 10 or 10' to close the loop, reaching

point 1 or 1'. We also see a decent match of the mean field approach with agent-based model (ABM) simulations [Figs. 4(c) and 4(d)].

We can interpret these results by posing the following question. Imagine that we can somehow influence the attitudes of the layers such that we soften the animosities towards a more amicable, and maybe even eventually slightly cordial,

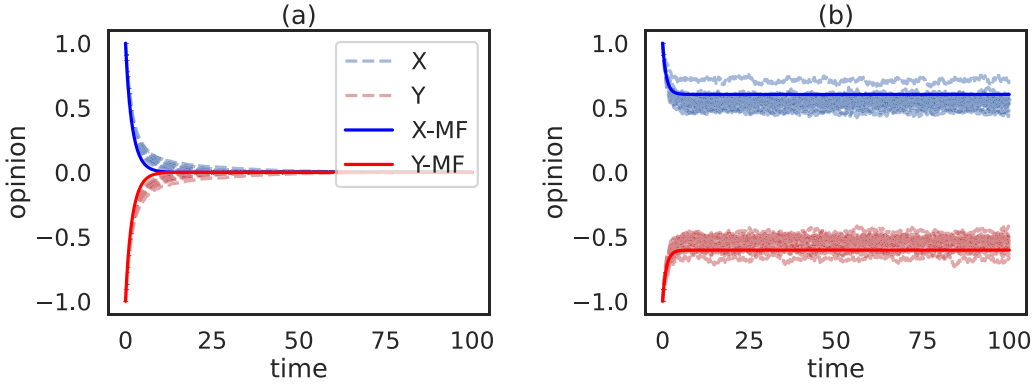


FIG. 6. Example trajectories of the groups' average opinions as they change in time. Dashed lines represent agent-based simulations, and 20 independent realizations are shown. Solid lines are the result of the mean field approximation (MF). (a) The behavior below the critical value with $\alpha = 0.84$; both groups converge on a neutral opinion. (b) The behavior above it with $\alpha = 4.0$; groups remain in their respective opinions in opposition to each other.

point of view. Would that be enough to settle a conflict of some sort? Or do we need to completely flip peoples' attitudes to make consensus possible? Our model suggests that softening attitudes can be enough, indeed. This implies that while prejudice can cause society to split, there is also room for hope because changes to attitudes that are not as drastic as one would, perhaps, expect can cause the layers to converge on an opinion, albeit not a neutral one.

Figure 5 presents solutions of Eq. (14) for different values of α . It is essential to note here that in this system we also face other critical behavior: in order to observe bistability for POL and OSR it is necessary that $\alpha > 1/(Kc)$ [see Figs. 5(a), 5(c) and 5(e)]. Otherwise, if starting from a polarized state for $\delta < 0$, the average opinion in both groups decreases with increasing δ , and when $\delta = -\frac{1}{Kc\alpha} + 1$, a state of neutral consensus is achieved, characterized by $x = 0$ and $y = 0$. The system stays in this state until $\delta = \frac{1}{Kc\alpha} - 1$, where both groups simultaneously acquire the same nonzero opinion (the OSR state). When $\alpha > 1/(Kc)$, we also obtain an auxiliary solution [marked by black dashed lines in Figs. 5(a)–5(d)], which is, however, always unstable and therefore plays no role in the dynamics.

Let us consider now in detail the case of symmetrically and negatively coupled opposing layers with small values of α [i.e., the setting shown in Figs. 5(e)–5(h)] and check it against the outcomes of the ABM. With the use of the mean field theory we expect a phase transition from a neutral consensus, where both groups converge at zero, to a polarized state where the layers remain in their respective opinions in opposition to one another, as the control value $c\alpha$ is increased. We choose not to use a single control parameter as the behavior of the system slightly changes depending on whether we modulate c or α .

We arrive at that prediction in the same way as before; that is, from the Jacobian matrix (15) of the system (14) we can acquire the eigenvalues $\lambda_{+,-}$,

$$\lambda_{+,-} = c\alpha K(1 \pm \delta) - 1. \quad (18)$$

We can then find a steady state solution in the polarized phase ($x_{t \rightarrow \infty} = -y_{t \rightarrow \infty}$) by numerically solving the following relation:

$$x_{t \rightarrow \infty} = (1 - \delta)Kc \tanh \alpha x_{t \rightarrow \infty}, \quad (19)$$

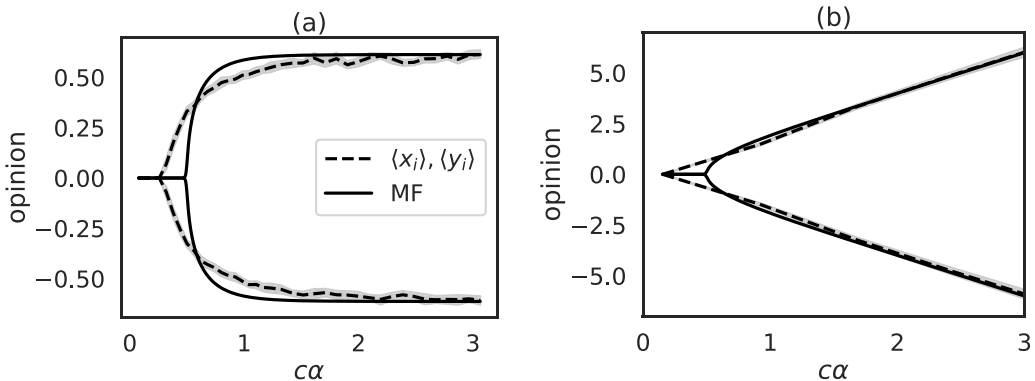


FIG. 7. Phase transition (a pitchfork bifurcation) from the symmetric consensus to the opposite values of opinions in different layers X and Y under different parameter modulations in both agent-based simulations and the mean field approximation. The transition takes place at the point $K(1 - \delta)c\alpha = 1$. (a) The transition as we increase α and keep $c \approx 0.306$. (b) The case when we keep $\alpha = 1$ and change c by increasing the parameter m . The agent-based results are averaged over 20 independent realizations with a 95% confidence interval present in the form of the error bands. Asymptotic behaviors observed in both panels for $c\alpha \gg 1$ are in very good agreement with Eq. (20).

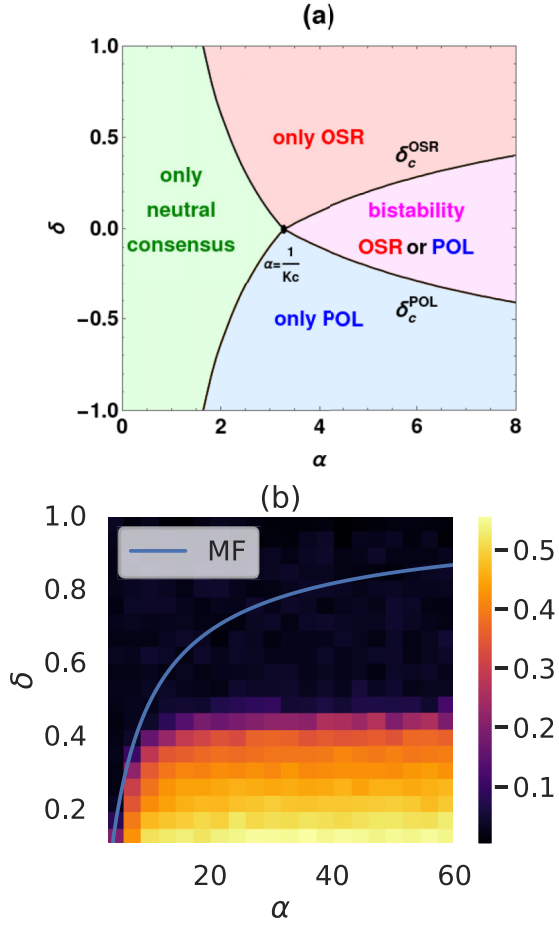


FIG. 8. (a) Phase diagram of the system given by Eq. (14) for $c = 0.306$ and $K = 1$. (b) Numerical simulations of the ABM model, where color shows $|\langle x \rangle - \langle y \rangle|$, with a visible transition from opposing opinions to a non-neutral consensus. In both panels solid lines come from the MF solution given by Eq. (17).

which can be written in the normalized form $u = K(1 - \delta)\alpha c \tanh(u)$ when $u = \alpha x_{t \rightarrow \infty}$. Since the solution u of the last equation increases from zero to $K(1 - \delta)\alpha c$ when the product $K(1 - \delta)\alpha c$ increases from 1 to ∞ , for $K(1 - \delta)\alpha c \gg 1$ the equation

$$x_{t \rightarrow \infty} \approx K(1 - \delta)c \quad (20)$$

explains the difference in the behavior we mentioned (c vs α modulation) and observe in Fig. 6.

In Fig. 7 we present examples of trajectories of the system where we arbitrarily chose groups to start with all their agents with opinion $+1$ (X) or with -1 (Y); however, the results do not depend on this choice. There we can see the two aforementioned phases, consensus and polarization. Plots show the mean opinion of each layer as a function of time. The agent-based simulations are not deterministic, and therefore, we show 20 independent realizations and compare them against the mean field prediction. It is apparent that below the critical value of $c\alpha$ the whole system converges at zero: both layers reach a neutral consensus [Fig. 7(a)]. As the control parameter is increased, the situation changes, and a polarization phase

occurs [Fig. 7(b)]. The two layers now stand in opposition to one another, and no consensus is possible.

Using the mean field theory, we estimate the critical value of $c\alpha$ and present the test of our predictions in Fig. 6. As mentioned before, it depends on whether we modulated α or c , and we show that in Figs. 6(a) and 6(b), respectively. When $c = \text{const}$, the system reaches a plateau; however, when c is increased, the final opinion value of the system also increases indefinitely. In both scenarios we see a phase transition (a supercritical pitchfork bifurcation [67]) at a certain critical value and a reasonably decent fit from the mean field approximation.

We find this setting to be representative of a typical echo-chamber situation in the context of two rivaling groups such as political parties. If the animosity of one for the other or of both mutually is strong enough, then no consensus is possible; while the groups may not be as radical as they were initially, they will always persist in their view opposite to the other. This essentially shows that prejudice has the potential to lock society into a predetermined antagonistic state.

The outcomes of this analysis can be summarized in a concise way with the $\delta - \alpha$ phase diagram shown in Fig. 8(a), where the predictions of different states of the systems (i.e., neutral consensus, polarization, radicalization, and bistability) are presented. We also see a decent match of the ABM results, but only for relatively small values of α and δ ; see Fig. 8(b), where we show a heat map of the $\delta - \alpha$ phase space in which the color denotes the distance between averages.

C. Nonsymmetric coupling

Let us now make a bridge between the systems (14) and (5) by formulating predictions in the mean field approach for the case when the coupling between layers is not symmetrical. At first we shall look at a scenario in which the coupling has the same sign but (possibly but not necessarily) different magnitudes; that is, we consider the system as described by (5) with the omission of the external bias. The procedure for the analysis of this system is, of course, analogous to what we already did before.

The Jacobian matrix of (5) is

$$J|_{\langle x \rangle = \langle y \rangle = 0} = \begin{bmatrix} -1 + c\alpha K & c\alpha K_{xy} \\ c\alpha K_{yx} & -1 + c\alpha K \end{bmatrix}, \quad (21)$$

from which we get both eigenvalues:

$$\lambda_{1,2} = c\alpha K \mp c\alpha \sqrt{K_{xy}K_{yx}} - 1. \quad (22)$$

When $K_{xy} = K_{yx}$, eigenvalues $\lambda_{1,2}$ reduce to $\lambda_{+,-}$,

$$\lambda_{+,-} = c\alpha(K \pm K_{xy}) - 1, \quad (23)$$

calculated directly from the agent-based model (3) in the limit $N \rightarrow \infty$, and in such a case the corresponding eigenvectors of Jacobian (21) are $e_+ = [1, 1]^T$ and $e_- = [1, -1]^T$.

In general the product $K_{xy}K_{yx}$ can be positive or negative; if it is positive, then either $K_{xy} > 0 \wedge K_{yx} > 0$, and the system falls into what was described by Baumann *et al.* (unless we consider the weak coupling $\delta < 1$ introduced in Sec. IV B), or $K_{xy} < 0 \wedge K_{yx} < 0$, and new behavior in the system emerges, accompanied by a phase transition occurring when $\lambda_{\max} = \lambda_-$ changes sign. Since the eigenvector e_- is asymmetrical, the case $\lambda_{\max} > 0$ means that the consensus

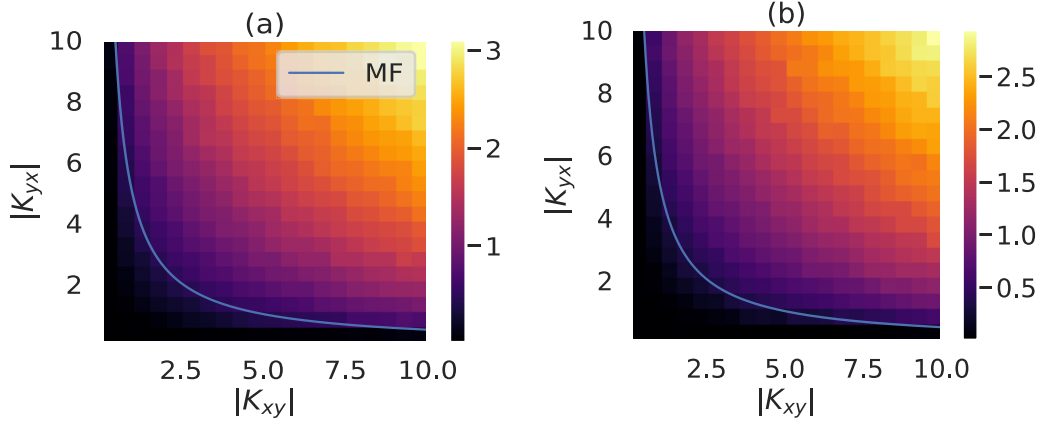


FIG. 9. The coupling parameter phase space $|K_{xy}| - |K_{yx}|$, when $K_{xy}, K_{yx} < 0$, in the form of a heat map, where the color represents the average $(1/2)(|\langle x_t \rangle| + |\langle y_t \rangle|)$, with a visible transition from neutral consensus to polarization. MF is Eq. (24). (a) Results for initial conditions corresponding to the opposite radicalization in each layer. (b) The initial conditions for all agents were drawn randomly from a uniform distribution $(-1, 1)$, showing that this result does not depend on initial conditions.

phase $x = y = 0$ loses its stability, and the systems are polarized; that is, opinions in groups X and Y split into opposite directions. From λ_{\max} changing its sign we get the following relationship between K_{xy} and K_{yx} :

$$K_{yx} = \left(\frac{1 - c\alpha K}{c\alpha} \right)^2 \frac{1}{K_{xy}}. \quad (24)$$

If $K_{yx} = K_{xy} < 0$ and the system is in the polarized phase, then its steady state is $x_{t \rightarrow \infty} = -y_{t \rightarrow \infty}$, which can be found by solving numerically for $x_{t \rightarrow \infty}$ in the following relation:

$$x_{t \rightarrow \infty} = (K - K_{xy})c \tanh(\alpha x_{t \rightarrow \infty}). \quad (25)$$

Equation (25) can be again written in a normalized form, as earlier $u = (K - K_{xy})\alpha c \tanh(u)$ when $u = \alpha x_{t \rightarrow \infty}$. Since the solution u of the last equation increases from zero to $(K - K_{xy})\alpha c$ when the product $(K - K_{xy})\alpha c$ increases from 1 to ∞ , for $(K - K_{xy})\alpha c \gg 1$,

$$x_{t \rightarrow \infty} \approx (K - K_{xy})c, \quad (26)$$

which also explains the difference in the behavior we observe in Fig. 6, albeit in a more general context.

We also present a heat map (Fig. 9) of the coupling parameter phase space with $Kc\alpha \approx 0.306$. The color there shows the

absolute value of the mean opinion of the system. Again, we see a transition from consensus to polarization, with a good match to the mean field approach and, specifically, Eq. (24).

Another interesting case is that of an asymmetric or perhaps even antisymmetric coupling in which one group “likes” the other but the feeling is not mutual; that is, the signs of the coupling parameters are opposite. According to the mean field theory, we ought to see two possible behaviors of the system: dampened or sustained oscillations depending on the values of the control parameter. As before the behavior does depend on whether we change c or α . In Figs. 10 and 11 we show time and phase trajectories, respectively. In both cases it is apparent that the two aforementioned behaviors are present. Namely, the system has two possible attractors: a point or an orbit. While there is a slight shift in when the transition occurs when comparing agent-based simulations and the mean field approximation, we find the analytical approach is qualitatively successful.

This effect is due to the product $K_{xy}K_{yx}$ being negative and then the eigenvalues being complex, and the system exhibits a supercritical Hopf bifurcation [67]. When $Kc\alpha < 1$, the attractor of dynamical system (5) is the point $(0,0)$; that is, there is a consensus among the groups. When $Kc\alpha > 1$, this trivial fixed point loses its stability, and we expect to see oscillations

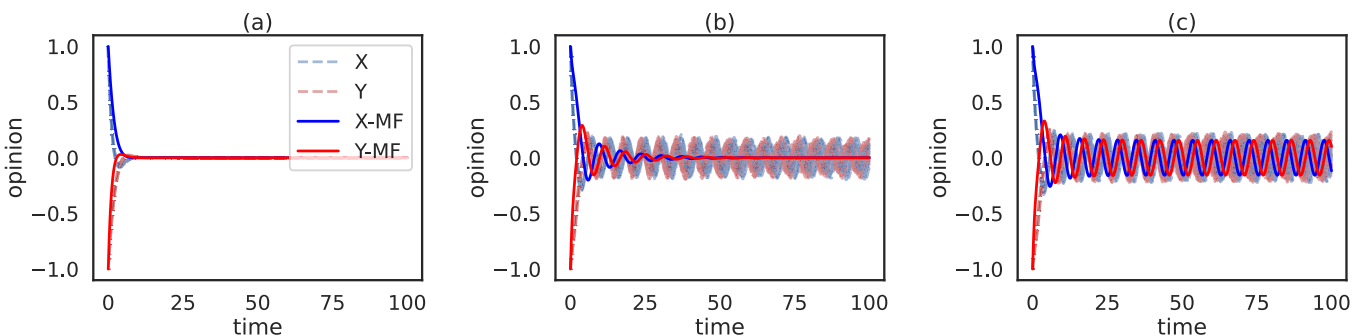


FIG. 10. Example trajectories in the asymmetric coupling parameter scenario for (a)–(c) $\alpha = 1, 3, 3.5$, respectively. Results of 20 independent agent-based simulations are shown as dashed lines, with solid lines representing the MF approximation. Two distinct behaviors are visible: sustained and dampened oscillations.

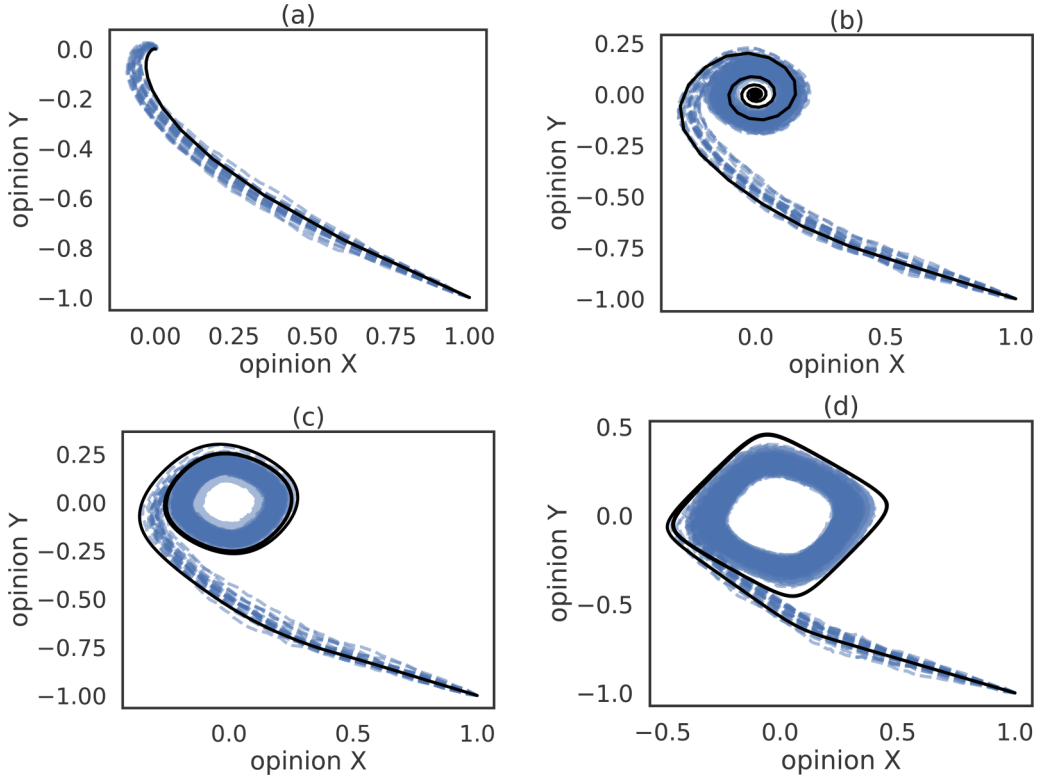


FIG. 11. $Y(X)$ trajectories in the asymmetric coupling scenario for (a)–(d) $\alpha = 1, 3, 4, 10$, respectively, with dashed lines representing 20 independent realizations of the agent-based simulation and solid lines showing the mean field solution. We observe in detail that the system has two possible attractors: a point and an orbit. For $Kc\alpha > 1$ the point $(0,0)$ becomes unstable, and trajectories starting from it would also end in an orbit.

in the system corresponding to a limit cycle attractor [the trajectory cannot diverge to infinity since the function $\tanh(x)$ is bounded].

What is also interesting in this case is how the sustained oscillations change as we modulate α or c . Like before, we choose to modulate c via the parameter m . In Fig. 12 we show both frequencies and amplitudes as functions of $c\alpha$ with either α or m modulation. A supercritical Hopf bifurcation takes place at the point $Kc\alpha = 1$, and the frequency of the emerging periodic orbit at the critical point should be equal to $f_{\text{crit}} = c\alpha\sqrt{K_{xy}K_{yx}}/2\pi \approx 0.1592$. Although the oscillations are highly nonlinear [due to the $\tanh(x)$ term], the mean field predictions show a good qualitative match to agent-based simulations. The frequency f is slightly different in the overcritical region compared to the critical value f_{crit} that is in agreement with the theory of Hopf bifurcation [68]. For large values of $c\alpha$ the amplitude of oscillations saturates as the function of the parameter α and is a linear function of the parameter c . This behavior is similar to plots in Fig. 6, and it is related to the scaling observed for the asymptotic steady state solution $x_{t \rightarrow \infty}$ [see Eq. (26)].

While this scenario might be slightly less obvious to interpret, we do believe there are certain parallels to be drawn here. It may seem as though one group is a *trend setter*, while the other group contains *followers*. In such a case there is a sort of feedback dynamic very similar to what we observe in our model. One group, the followers, is positively oriented towards the other, the trend setters, as they look up to them and would like to be, act, and think like them. On the other

hand, the trend setters share a negative attitude towards the followers in this context. While they might appreciate the following, they would very much want to move away from it in terms of the opinion in question. This leads to this chasing and oscillating behavior. However, if the magnitudes of the attitudes *within* the groups are not strong enough, the dynamic simply dies down because the followers are not interested in following and the trend setters are not interested in trend setting.

V. CONCLUSIONS

In this paper we considered a temporal bilayer echo-chamber and polarization model on complex networks inspired by the monolayer model introduced by Baumann *et al.* We recognize that there is both a precedent and apparent value in studying scenarios in which two clear-cut groups—or layers in a network—interact with one another. Understanding how layered complex networks evolve in various environments in the context of opinion dynamics can help us better prepare for studying in detail such prominent real-world social phenomena as misinformation campaigns and echo chambers.

We formulated the dynamics equations for the bilayer system (3) and then provided a mean field analysis that uncovered interesting possible scenarios. The nature of system's behavior is different depending on the coupling between the layers. We categorized those couplings as symmetric and non-symmetric with the special case of added external bias also

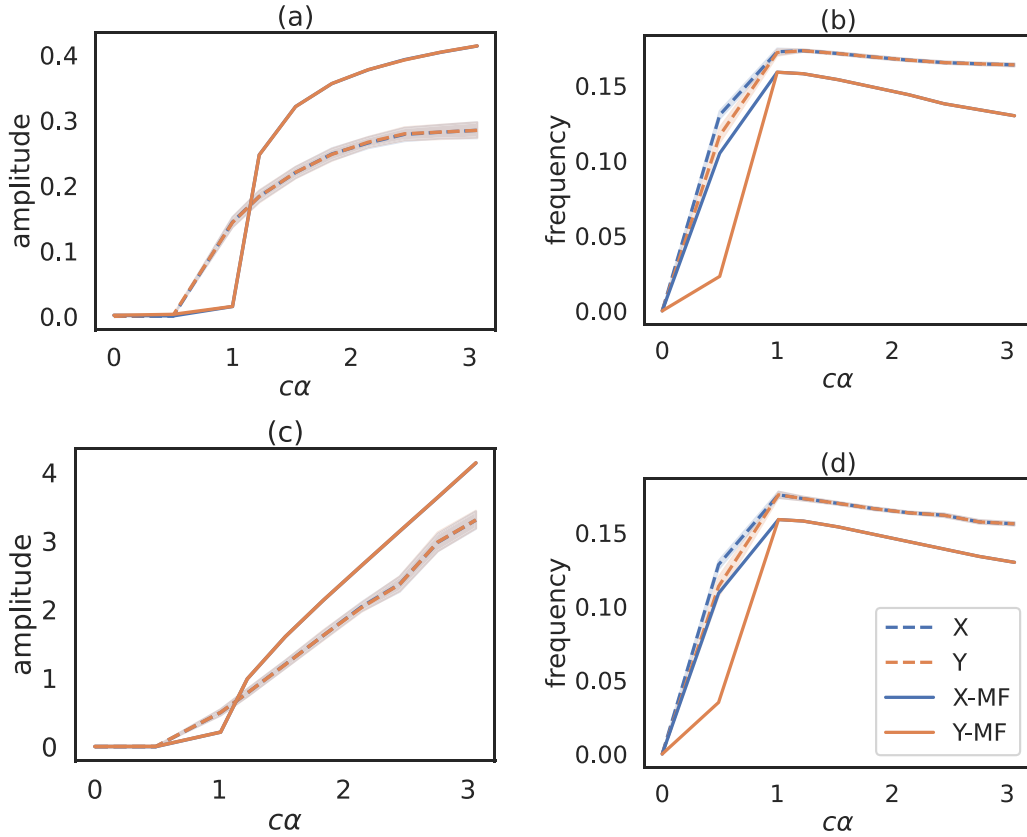


FIG. 12. The oscillation frequencies and amplitude dependence on the parameter modulation in the asymmetric coupling case. The top row is for α modulation, and the bottom one is for m . Dashed lines represent an average over 20 independent realizations of agent-based simulations, with the 95% confidence interval present as the error bands. Solid lines show the mean field solution. Differences in asymptotic behaviors of amplitudes in (a) and (c) are similar to differences observed for values of the steady-state solutions $x_{t \rightarrow \infty}$ in Figs. 6(a) and 6(b).

considered. In more detail there are a negative symmetric case in which the groups do not like each other; opinion oscillations in which one group likes the other but the feeling is not mutual; the aforementioned external bias, where we consider the other group to be an external bias acting upon a monolayer system; and, finally, a weak positive coupling in which there is an attraction between the groups that is, however, not as strong as the attraction within them.

When the two layers were weakly yet positively coupled, we saw that a critical value of the coupling parameter that causes the system to experience a sudden shift in the opinions exists. In this case we observed that there is a transition from a polarized state to a one-sided consensus (or a radicalized state) in which all agents (from both layers) share a similar and nonzero opinion. Similar to the previous case, the match between the mean field theory and simulations is qualitatively satisfying; however, for larger values of the control parameter the predictions about when the transition should happen diverge from the results for numerical experiments.

In the opposite polarization scenario, i.e., negative symmetric, we observed that the coexistence of two groups with different (opposite) opinions is possible. The system undergoes a phase transition from a neutral consensus, in which the two layers' opinions merge at zero, to a polarized state, in which the two groups coexist, each of them having their own opinion that is the opposite of that of the other group.

The details of this pitchfork bifurcation and the asymptotic behavior of the system depend on whether we modulate the nonlinearity parameter α or the combined social influence parameter c or the coupling parameters K_{xy} and K_{yx} ; however, in both cases the mean field approximation gives us a satisfying fit to agent-based simulations.

In the case of a single layer with an external bias present we postulated that it might be possible to model either a background of some sort or the second layer for that matter as simply a cumulative effect in the form of such an external bias. We found that the behavior here is not very dissimilar to the weak positive coupling scenario. Namely, there exists a critical value of said bias at which, when the system is subject to it, a sudden change to the opposite opinion is possible and the cusp catastrophe is apparent. For small values of the control parameter we found a decent match between the mean field approach and agent-based simulations; however, for larger values the two diverge in the prediction about when the transition should occur, most likely due to the finite size of the simulated system.

Finally, when the coupling parameters were set antisymmetrically, in the sense that one is positive and one is negative, we detected a transition from dampened to sustained oscillations of the layers' opinions: a supercritical Hopf bifurcation. In a way one might say that one group is "chasing" the other with their opinions, while the other is trying to get away.

We additionally found that the oscillations are highly non-linear as the frequency *decreases* with the control parameter as opposed to *increasing* as one would expect from a linear oscillator. At the same time the amplitude increases with the control parameter. We believe the amplitude here plays the role of a sort of barrier for the system to overcome, so the higher the barrier is, the longer it takes to overcome it; thus, the frequency of the oscillations increases.

With each scenario we have drawn parallels to the real world to illustrate what these results could mean for understanding the dynamics of our societies. We understand that there are limitations with both the model and the approach in general because it can often be difficult to

construct reproducible experiments in a sociological context; however, we firmly believe that seeing where certain assumptions can lead us is an important and crucial building block of science.

ACKNOWLEDGMENTS

This research was supported by an IDUB against COVID-19 project granted by Warsaw University of Technology under the program Excellence Initiative: Research University (IDUB). J.A.H. was partially supported by the Russian Science Foundation, Agreement No. 17-71-30029 with cofinancing of Bank Saint Petersburg.

-
- [1] J. A. Hołyst, K. Kacperski, and F. Schweitzer, Social impact models of opinion dynamics, *Ann. Rev. Comput. Phys.* **9**, 253 (2001).
- [2] C. Castellano, S. Fortunato, and V. Loreto, Statistical physics of social dynamics, *Rev. Mod. Phys.* **81**, 591 (2009).
- [3] S. Galam, *Sociophysics: A Physicist's Modeling of Psychological Phenomena* (Springer, Boston, MA, 2016).
- [4] S. Galam, Modeling the forming of public opinion: An approach from sociophysics, *Global Econ. Manage. Rev.* **18**, 2 (2013).
- [5] P. Sen and B. K. Chakrabarti, *Sociophysics: An Introduction* (Oxford University Press, Oxford, 2014).
- [6] F. Baumann, P. Lorenz-Spreen, I. M. Sokolov, and M. Starnini, Modeling Echo Chambers and Polarization Dynamics in Social Networks, *Phys. Rev. Lett.* **124**, 048301 (2020).
- [7] W. Cota, S. C. Ferreira, R. Pastor-Satorras, and M. Starnini, Quantifying echo chamber effects in information spreading over political communication networks, *EPJ Data Sci.* **8**, 35 (2019).
- [8] P. Törnberg, Echo chambers and viral misinformation: Modeling fake news as complex contagion, *PLoS ONE* **13**, e0203958 (2018).
- [9] K. Sasahara, W. Chen, H. Peng, G. L. Ciampaglia, A. Flammini, and F. Menczer, Social influence and unfollowing accelerate the emergence of echo chambers, *J. Comput. Soc. Sci.* **4**, 381 (2020).
- [10] M. Del Vicario, A. Bessi, F. Zollo, F. Petroni, A. Scala, G. Caldarelli, H. E. Stanley, and W. Quattrociocchi, The spreading of misinformation online, *Proc. Natl. Acad. Sci. USA* **113**, 554 (2016).
- [11] S. Vosoughi, D. Roy, and S. Aral, The spread of true and false news online, *Science* **359**, 1146 (2018).
- [12] A. Bessi, F. Zollo, M. Del Vicario, A. Scala, G. Caldarelli, and W. Quattrociocchi, Trend of narratives in the age of misinformation, *PLoS ONE* **10**, e0134641 (2015).
- [13] C. Shao, P.-M. Hui, L. Wang, X. Jiang, A. Flammini, F. Menczer, and G. L. Ciampaglia, Anatomy of an online misinformation network, *PLoS ONE* **13**, e0196087 (2018).
- [14] C. Shao, G. L. Ciampaglia, A. Flammini, and F. Menczer, Hoaxy, in *Proceedings of the 25th International Conference Companion on World Wide Web—WWW '16 Companion* (International World Wide Web Conferences Steering Committee, Montréal, Québec, Canada, 2016), pp. 745–750.
- [15] C. Shao, G. L. Ciampaglia, O. Varol, K.-C. Yang, A. Flammini, and F. Menczer, The spread of low-credibility content by social bots, *Nat. Commun.* **9**, 4787 (2018).
- [16] P. DiMaggio, J. Evans, and B. Bryson, Have American's social attitudes become more polarized? *Am. J. Soc.* **102**, 690 (1996).
- [17] M. P. Fiorina and S. J. Abrams, Political polarization in the american public, *Annu. Rev. Polit. Sci.* **11**, 563 (2008).
- [18] T. Mouw and M. E. Sobel, Culture wars and opinion polarization: The case of abortion, *Am. J. Sociol.* **106**, 913 (2001).
- [19] A. M. McCright and R. E. Dunlap, The politicization of climate change and polarization in the American public's views of global warming, 2001-2010, *Soc. Q.* **52**, 155 (2011).
- [20] T. Z. Lin and X. Tian, Audience design and context discrepancy: How online debates lead to opinion polarization, *Symb. Interact.* **42**, 70 (2019).
- [21] M. D. Conover, J. Ratkiewicz, M. Francisco, B. Gonçalves, A. Flammini, and F. Menczer, Political polarization on Twitter, in *Proceedings of the Fifth International AAAI Conference on Weblogs and Social Media* (AAAI Press, Menlo Park, CA, 2021), Vol. 5, pp. 89–96.
- [22] M. D. Conover, B. Gonçalves, A. Flammini, and F. Menczer, Partisan asymmetries in online political activity, *EPJ Data Sci.* **1**, 6 (2012).
- [23] A. Hanna, C. Wells, P. Maurer, L. Friedland, D. Shah, and J. Matthes, Partisan alignments and political polarization online: A computational approach to understanding the French and US presidential elections, in *Proceedings of the 2nd Workshop on Politics, Elections and Data: PLEAD '13* (ACM Press, New York, 2013), pp. 15–22.
- [24] W. J. Brady, J. A. Wills, J. T. Jost, J. A. Tucker, and J. J. Van Bavel, Emotion shapes the diffusion of moralized content in social networks, *Proc. Natl. Acad. Sci. USA* **114**, 7313 (2017).
- [25] I. Weber, V. R. K. Garimella, and A. Batayneh, Secular vs. Islamist polarization in Egypt on Twitter, in *Proceedings of the 2013 IEEE/ACM International Conference on Advances in Social Networks Analysis and Mining* (ACM Press, New York, NY, 2013), pp. 290–297.
- [26] F. Baumann, P. Lorenz-Spreen, I. M. Sokolov, and M. Starnini, Emergence of Polarized Ideological Opinions in Multidimensional Topic Spaces, *Phys. Rev. X* **11**, 011012 (2021).
- [27] S. Schweighofer, F. Schweitzer, and D. Garcia, A weighted balance model of opinion hyperpolarization, *J. Artif. Soc. Soc. Simul.* **23**, 5 (2020).

- [28] T. Chen, Q. Li, J. Yang, G. Cong, and G. Li, Modeling of the public opinion polarization process with the considerations of individual heterogeneity and dynamic conformity, *Mathematics* **7**, 917 (2019).
- [29] T. Kurahashi-Nakamura, M. Mäs, and J. Lorenz, Robust clustering in generalized bounded confidence models, *J. Artif. Soc. Soc. Simul.* **19**, 7 (2016).
- [30] S. Banisch and E. Olbrich, Opinion polarization by learning from social feedback, *J. Math. Soc.* **43**, 76 (2019).
- [31] M. Macy, S. Deri, A. Ruch, and N. Tong, Opinion cascades and the unpredictability of partisan polarization, *Sci. Adv.* **5**, 245 (2019).
- [32] P. J. Górski, K. Bochenina, J. A. Hołyst, and R. M. D'Souza, Homophily Based on Few Attributes Can Impede Structural Balance, *Phys. Rev. Lett.* **125**, 078302 (2020).
- [33] D. Waldner and E. Lust, Unwelcome change: Coming to terms with democratic backsliding, *Annu. Rev. Polit. Sci.* **21**, 93 (2018).
- [34] K. Wiesner, A. Birdi, T. Eliassi-Rad, H. Farrell, D. Garcia, S. Lewandowsky, P. Palacios, D. Ross, D. Sornette, and K. Thébault, Stability of democracies: A complex systems perspective, *Eur. J. Phys.* **40**, 014002 (2018).
- [35] K. Suchecki and J. A. Hołyst, Ising model on two connected Barabasi-Albert networks, *Phys. Rev. E* **74**, 011122 (2006).
- [36] K. Suchecki and J. A. Hołyst, Bistable-monostable transition in the Ising model on two connected complex networks, *Phys. Rev. E* **80**, 031110 (2009).
- [37] T. Krueger, J. Szubiński, and T. Weron, Conformity, anticonformity and polarization of opinions: Insights from a mathematical model of opinion dynamics, *Entropy* **19**, 371 (2017).
- [38] A. Chmiel and K. Sznajd-Weron, Phase transitions in the q -voter model with noise on a duplex clique, *Phys. Rev. E* **92**, 052812 (2015).
- [39] J. Choi and K.-I. Goh, Majority-vote dynamics on multiplex networks with two layers, *New J. Phys.* **21**, 035005 (2019).
- [40] R. Lambiotte and M. Ausloos, Coexistence of opposite opinions in a network with communities, *J. Stat. Mech.* (2007) P08026.
- [41] R. Lambiotte, M. Ausloos, and J. A. Hołyst, Majority model on a network with communities, *Phys. Rev. E* **75**, 030101(R) (2007).
- [42] A. Chmiel, J. Sienkiewicz, and K. Sznajd-Weron, Tricriticality in the q -neighbor Ising model on a partially duplex clique, *Phys. Rev. E* **96**, 062137 (2017).
- [43] A. Chmiel, J. Sienkiewicz, A. Fronczak, and P. Fronczak, A veritable zoology of successive phase transitions in the asymmetric q -voter model on multiplex networks, *Entropy* **22**, 1018 (2020).
- [44] K. T. Gradoń, J. A. Hołyst, W. R. Moy, J. Sienkiewicz, and K. Suchecki, Countering misinformation: A multidisciplinary approach, *Big Data Soc.* **8**, 20539517211013848 (2021).
- [45] Y. Ye, Q. Zhang, Z. Ruan, Z. Cao, Q. Xuan, and D. D. Zeng, Effect of heterogeneous risk perception on information diffusion, behavior change, and disease transmission, *Phys. Rev. E* **102**, 042314 (2020).
- [46] L. G. Alvarez-Zuzek, C. E. La Rocca, J. R. Iglesias, and L. A. Braunstein, Epidemic spreading in multiplex networks influenced by opinion exchanges on vaccination, *PLoS ONE* **12**, e0186492 (2017).
- [47] N. F. Johnson, N. Velásquez, N. J. Restrepo, R. Leahy, N. Gabriel, S. El Oud, M. Zheng, P. Manrique, S. Wuchty, and Y. Lupu, The online competition between pro- and anti-vaccination views, *Nature (London)* **582**, 230 (2020).
- [48] M. Mäs and A. Flache, Differentiation without distancing. Explaining bi-polarization of opinions without negative influence, *PLoS ONE* **8**, e74516 (2013).
- [49] B. Jayles, H.-R. Kim, R. Escobedo, S. Cezera, A. Blanchet, T. Kameda, C. Sire, and G. Theraulaz, How social information can improve estimation accuracy in human groups, *Proc. Natl. Acad. Sci. USA* **114**, 12620 (2017).
- [50] H. Sompolinsky, A. Crisanti, and H. J. Sommers, Chaos in Random Neural Networks, *Phys. Rev. Lett.* **61**, 259 (1988).
- [51] E. Eldar, J. D. Cohen, and Y. Niv, The effects of neural gain on attention and learning, *Nat. Neurosci.* **16**, 1146 (2013).
- [52] N. Perra, B. Gonçalves, R. Pastor-Satorras, and A. Vespignani, Activity driven modeling of time varying networks, *Sci. Rep.* **2**, 469 (2012).
- [53] M. Starnini and R. Pastor-Satorras, Topological properties of a time-integrated activity-driven network, *Phys. Rev. E* **87**, 062807 (2013).
- [54] A. Moinet, M. Starnini, and R. Pastor-Satorras, Burstiness and Aging in Social Temporal Networks, *Phys. Rev. Lett.* **114**, 108701 (2015).
- [55] S. Liu, N. Perra, M. Karsai, and A. Vespignani, Controlling Contagion Processes in Activity Driven Networks, *Phys. Rev. Lett.* **112**, 118702 (2014).
- [56] P. Holme and M. E. J. Newman, Nonequilibrium phase transition in the coevolution of networks and opinions, *Phys. Rev. E* **74**, 056108 (2006).
- [57] D. Kimura and Y. Hayakawa, Coevolutionary networks with homophily and heterophily, *Phys. Rev. E* **78**, 016103 (2008).
- [58] D. C. Mattis, *The Theory of Magnetism I: Statics and Dynamics*, Solid-State Sciences Vol. 17 (Springer, Berlin, Heidelberg, 2012).
- [59] D. G. Myers and H. Lamm, The group polarization phenomenon, *Psychol. Bull.* **83**, 602 (1976).
- [60] D. J. Isenberg, Group polarization: A critical review and meta-analysis, *J. Pers. Soc. Psychol.* **50**, 1141 (1986).
- [61] J. Dormand and P. Prince, A family of embedded Runge-Kutta formulae, *J. Comput. Appl. Math.* **6**, 19 (1980).
- [62] P. Virtanen *et al.*, SciPy 1.0: Fundamental algorithms for scientific computing in python, *Nat. Methods* **17**, 261 (2020).
- [63] J. A. Krosnick, Attitude importance and attitude change, *J. Exp. Soc. Psychol.* **24**, 240 (1988).
- [64] E. C. Zeeman, Catastrophe theory, in *Structural Stability in Physics* (Springer, Berlin, Heidelberg, 1979), pp. 12–22.
- [65] V. I. Arnol'd, *Catastrophe Theory* (Springer, Berlin, Heidelberg, 2003).
- [66] A. M. Lyapunov, The general problem of the stability of motion, *Int. J. Control* **55**, 531 (1992).
- [67] S. H. Strogatz, *Nonlinear Dynamics and Chaos with Student Solutions Manual: With Applications to Physics, Biology, Chemistry, and Engineering* (CRC Press, Boca Raton, FL, 2018).
- [68] E. Ott, *Chaos in Dynamical Systems* (Cambridge University Press, Cambridge, 2002).